AL-Bahir
Journal for Engineering and Pure Sciences
BJEPS

Manuscript 1101

Analysis of photonic crystal fiber for terahertz applications in optical communications

Hiba Noori

Rasha A. Hussein

Muwafaq F. Jaddoa

ORIGINAL STUDY

Analysis of Photonic Crystal Fiber for Terahertz Applications in Optical Communications

Hiba Noori*, Rasha A. Hussein, Muwafaq F. Jaddoa

Department of Physics/College of Science, Al-Muthanna University, Samawah, Iraq

Abstract

This study discusses photonic crystal fibers (PCFs), a novel type of optical waveguide that performs noticeably better than traditional optical fibers and offers an extraordinary light-guiding mechanism. In this work, a porous core PCF was designed and analyzed. The fiber has a core of 360 μm diameter surrounded by four circular rings of air holes. COMSOL Multiphysics is used to simulate the suggested PCF. By altering two crucial structural components—the pitch spacing, which ranges from 165 to 175 μm, and the diameter (d), which ranges from 140 to 160 μm—the fiber behavior was investigated at frequencies ranging from 0.9 to 1.4 THz. The results demonstrate that dispersion properties exhibit strong dependence on diameter variations, particularly at d = 160 μm. Analysis of the effective area (A_{eff}) reveals that it is inversely proportional to frequency, with maximum values observed at d = 140, reaching 11.5×10^{-7} m^2. The different effective mode indices of our proposed PCFs are investigated when the diameter d is modified. It can be seen from the results that the effective mode index shows significant sensitivity to the variation of the diameter d, When d = 140 μm, the effective mode index shows the highest values starting from 1.29 and reaching 1.38, while d = 160 μm shows the lowest values ranging from 1.23 to 1.35. The medium diameter d = 150 μm exhibits intermediate values throughout the frequency range. This indicates that the effective mode index changes significantly with diameter variations. The reported design has lower dispersion than the previously reported researches and lower effective area which in turn refer to higher nonlinearity. Hence the suggested design can be used for supercontinuum generation. It is possible to fabricate the proposed PCFs by employing the widely utilized sol-gel casting, drilling, and stack and draw techniques. The PCF demonstrates exceptional stability across its operational bandwidth, making it ideal for advanced terahertz sensing and communication applications.

Keywords: Photonic crystal fiber, Terahertz, Dispersion, Nonlinearity, Effective mode index

1. Introduction

Terahertz (THz) radiation, which falls between 0.1 and 10 THz, has garnered a lot of attention lately because of its many uses in electromagnetic radiation. The THz frequency range between the microwave and infrared (IR) portions of the electromagnetic spectrum (ES) [1–3]. THz communication systems present several distinctive advantages over traditional microwave communication methods. These include broader bandwidth capacity, higher carrier frequencies, enhanced information transmission capabilities, and superior penetration characteristics. Notably, THz systems require less complex tracking and aiming mechanisms compared to laser communication platforms, while maintaining robust performance [4]. The atmospheric absorption of THz radiation, provides an inherent security feature for space-based communications, making it particularly attractive for secure data transmission applications [5]. The scientific community has witnessed significant progress in THz technology research, particularly in imaging, sensing, detection, and radiation source development [6,7], hollow-core photonic crystal fibers and polymer fibers can be used for THz communication [10]. Because of their structural adaptability and necessary optical qualities, including high core power fraction, reduced effective material loss, lower dispersion, lower bending loss, and strong nonlinearity, porous core PCFs have garnered a lot of attention lately [1–6]. PCFs can be divided into

Received 15 February 2025; revised 28 April 2025; accepted 3 May 2025.
Available online 14 August 2025

* Corresponding author.
E-mail address: Sci.hiba@mu.edu.iq (H. Noori).

https://doi.org/10.55810/2313-0083.1101

two primary categories: index guiding PCF and photonic bandgap (PBG) guiding PCF. The modified total internal reflection method (MTIR) is used to guide light in index guiding PCF because the cladding region's effective refractive index is lower than the core region's [8]. The PBG effect, on the other hand, guides light if the core refractive index is lower than that of the cladding region [9].

The basic materials for a PCF's core can be any of several polymers guiding properties, including Topas, tellurite, Zeonex, graphene, Teflon, etc., [7,8]. TOPAS (cyclic olefin copolymer) demonstrates exceptionally low dispersion in the THz frequency range (0.1–1.0 THz), with a nearly constant refractive index of approximately 1.53 across this spectrum. This property is critical for maintaining signal integrity in broadband THz systems. Additionally, TOPAS exhibits remarkably low material absorption loss.

Two key research gaps had been identified: First, designs struggle to simultaneously achieve low losses and high flexibility. Nielsen et al. [10] demonstrated bendable TOPAS fibers but with relatively high losses (0.12 cm^{-1}), while Atakaramians et al. [11] achieved lower losses (0.06 cm^{-1}) but with significantly reduced mechanical flexibility, making field deployment challenging, second, fabrication complexity presents a significant barrier. Anthony et al. [12] demonstrated promising hollow-core structures but with complex manufacturing processes that limit scalability and increase production costs.

Our proposed porous ring-core structural configuration that achieves to the best of our knowledge the lowest reported material losses while maintaining exceptional flexibility A simplified fabrication approach using optimized TOPAS material that reduces manufacturing complexity and cost.

Mohamed Farhat O. Hameed et al. [13] THz photonic crystal fiber (PCF) polarization rotator (PR) is introduced. The suggested PCF-PR has an asymmetric porous core to decrease the material losses and increase the hybridness of the two polarized modes. Therefore, high polarization conversion ratio of 80.7 % is achieved with a good crosstalk of −18.9 dB at a frequency of 1 THz along a device length of 7.9 mm. Further, the operating frequency has a tolerance of f = 1 ± 0.1 THz where the crosstalk is still better than −15 dB. K. Yakasai [14] a highly birefringent photonic crystal fibre. It has been demonstrated that high birefringence of 0.08 can be achieved with low effective material loss of 0.03 cm^{-1} at 1.3 THz. Moreover, it has been shown that about 42 % of useful power flows through the elliptical core air holes. Near-zero flattened dispersion of 1.18 ± 0.01 ps/THz/cm is obtained for the x-polarization mode of the fibre.

B Kuiri et al. [15] SF2 doped ring core C-PCF with three layers of air holes is proposed. The PCF operates in 1–3 THz range with $>10^{-4}$ mode index separation. FEM optimization yields 98 stable OAM modes with purity >0.86. The design achieves ultra-low confinement loss ($<10^{-11}$ dB/cm), high effective mode area (>0.1 mm^2) and low dispersion (<0.02 ps/THz/cm), making it suitable for next-generation THz applications. B Kuiri et al. [16] polymer-based ring-core C-PCF is proposed. The fiber consists of Topas background, high refractive index Kapton ring and four air hole layers. FEM optimization yields 242 stable OAM modes near 1.9 THz with purity >0.9. The design achieves low CL (~10^{-9} dB/cm), large effective mode area (~10^{-2} mm^2), low dispersion (<1 ps/THz/cm) and high Δneff ($>10^{-3}$) across 1.5–3.5 THz. The fiber supports stable modes over wider spectrum than previous studies, making it suitable for next-generation THz multimode communication systems.

A circular porous-core PCF using TOPAS as the background material was introduced in this study. The cladding consists of air holes arranged in a circular structure with constant diameters and the hole-pitch was kept constant, the cladding's air-filling portion is intended to be greater than the core's. Consequently, it produces index contrast to keep the THz waves inside the waveguide, with these modifications in the profile, we were able to generate a large effective modal area along with a low confinement loss, thus making it useful for high power applications.

2. Numerical results

The whole vector nature of light has been taken into account by Maxwell's equation which explains how light behaves in PCF. For the magnetic field H, the vector wave equation is obtained as;

$$\nabla \times \left(\varepsilon^{-1}\nabla \times H\right) - \omega^2 \mu_o H = 0 \quad (1)$$

"The angular frequency is represented by (ω) the space permeability by μ, and the waveguide material's permittivity by ε. Using the vector wave equation and the magnetic field zero divergence condition, the whole vector eigenvalue equation can be derived" [14,15]:

$$[K]\{H\} - \beta^2[M]\{H\} = \{0\} \quad (2)$$

"where [H] is the global magnetic field vector, is the null vector, β is the propagation constant, and (K) and (M) are the global stiffness and mass

matrices. Furthermore, since neff = β/k, where k is the free space wave number, the effective index (neff) of the guided modes is computed from β".

"Dispersion and nonlinear effects influence the shape and spectrum of the optical pulses as they travel through the fiber. The definitions of the GVD and nonlinear parameters are as follows":

$$\gamma = \frac{2\pi n_2}{\lambda A_{eff}} \tag{3}$$

$$\beta_2 = -\frac{\lambda^2}{2\pi c} D \tag{4}$$

where n_2 is the Kerr nonlinear index, Aeff is the effective_mode Area. C, is the speed of light, and D, is the dispersion parameter which is given by:

$$D = -\frac{\lambda}{c}\frac{\partial^2}{\partial \lambda^2}\mathrm{Re}(n_{eff}) \tag{5}$$

3. Design and numerical results

The proposed PCF cross section is shown in Fig. (1). The design has four rings of air holes. Each cladding air hole has the same diameter (d) and is spaced with a hole pitch of Λ = 170 μm. There are round air holes in the porous core. The entire proposed PCF host background material is "TOPAS, also referred to as a cyclic-olefin copolymer in science, due to its unique and useful qualities, such as its flexibility in production to reach high glass transition temperatures, decency for biosensing, and insensitivity to dampness. The bulk material loss of TOPAS is 0.06 cm^{-1} at 0.4 THz and increases at a rate of 0.36 cm^{-1}/THz. It also has a relatively consistent refractive index of (1.525) over a broad frequency range of (0.1–2) THz with a lower material absorption loss and dispersion. The simulation accounts for the frequency-dependent nature of TOPAS's absorption coefficient".

Using the FV-FEM [24] with PML boundary condition [25,26], numerical results are produced, including the stated design's dispersion and nonlinearity. The suggested PCF n_{eff} and A_{eff} with frequency are also examined.

Fig. 2 shows the effect of diameter change on the nonlinearity characteristics of the proposed fiber, in this study the hole pitch is fixed to 170 μm and the three different diameters of 140, 150, and 160 μm, Analyzing the values determined at 1 THz, it can be revealed that the diameter of 140 μm shows the lowest nonlinearity of about 0.27$W^{-1}m^{-1}$, while the diameter of 150 μm shows a moderate nonlinearity value of about 0.31 $W^{-1}m^{-1}$, and the diameter of 160 μm exhibits the highest nonlinearity of about 0.33 $W^{-1}m^{-1}$.

Fig. 3 shows the effect of hole-pitch (Λ) variation on the nonlinear characteristics of optical fibers, in this investigation the diameter (d) = 150 μm, and three different hole-pitch values of (165, 170, and 175) μm. Has been used Analyzing the values determined at 1 THz, it can be revealed that at Λ = 175 μm a nonlinear value of about 2.83×107 W^{-1} m^{-1} is obtained while at Λ = 170 μm gives appoxirnatly the same value of about 3.16×107 W^{-1} m^{-1}, and at Λ = 165 μm shows a slightly higher nonlinear value of about 3.21×107 W^{-1} m^{-1}.

Fig. 4 shows the effect of diameter variation on the dispersion characteristics of the suggested design fibers, pitch (Λ) = 170, and three different diameters of (140, 150, and 160) micrometers, across a frequency range from 0.9 to 1.4 THz. Analyzing the

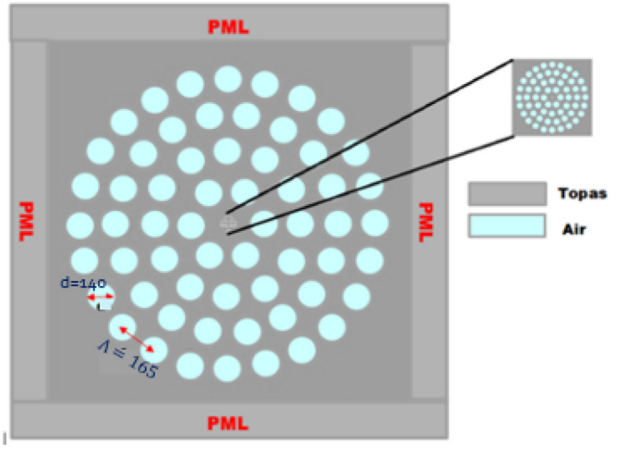

Fig. 1. Cross section of the proposed porous core THz fiber using TOPAS as the background. Diameter (d = 140 μm) and (pich = 165 μm).

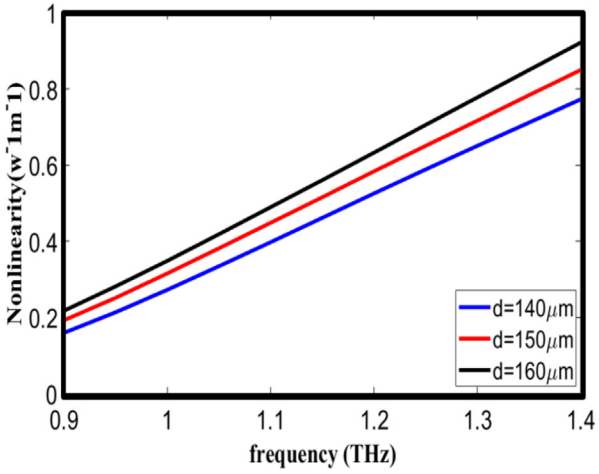

Fig. 2. Changes of the Nonlinearity parameter of the suggested PCF with Frequency at different (d = 140 μm, 150 μm, and 160 μm).

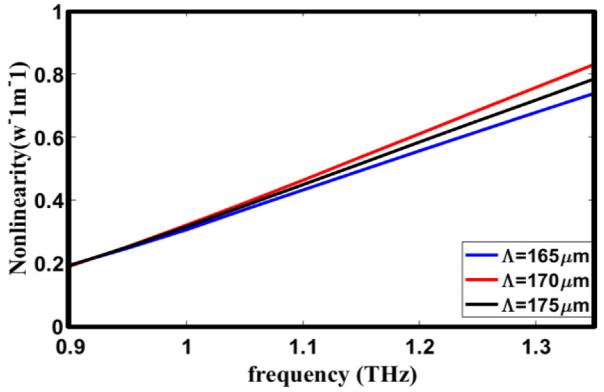

Fig. 3. Changes of the nonlinearity parameter of the suggested (PCF) with frequency at different (pitch = 165 μm, 170 μm, and 175 μm).

values determined at 1 THz, we find that diameter = 160 μm shows dispersion value of about 1.9 × 10^6 ps/(km·nm), while diameter = 150 shows higher value of about 1.1 × 10^6 ps/(km·nm), and diameter =140 μm shows dispersion value of about 0.25 × 10^6 ps/(km·nm).

Fig 5 shows the effect of pitch (Λ) variation on the dispersion characteristics of the optical fiber, refractive index (n) equals 1.523, diameter (d) equals 150 micrometers, and three different pitch values of (165, 170, and 175) micrometers. Analyzing the values determined at 1 THz, it can be revealed that the 175-micrometer pitch shows the highest dispersion value of approximately 1.7×10^6 ps/(km·nm), while the 170-micrometer pitch shows a moderate value of about 1.2×10^6 ps/(km·nm), whereas the 165-micrometer pitch exhibits the lowest dispersion of around 0.3×10^6 ps/(km·nm).

Fig. 6 shows the effect of diameter variation on the effective area characteristics of optical fibers, pitch (Λ) = 170 μm, and three different diameters of (140, 150, and 160 μm). Analyzing the values determined at a frequency of 1 THz, it can be revealed that the

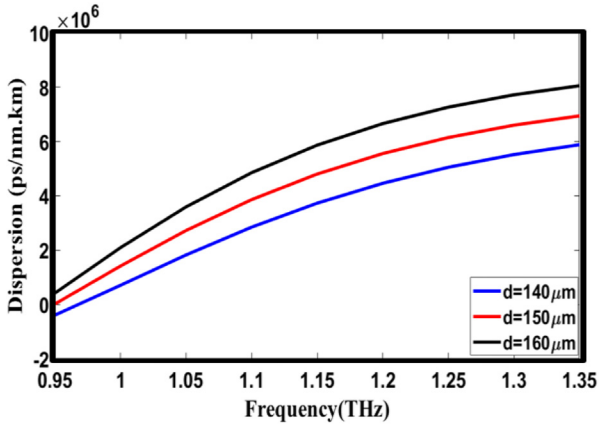

Fig. 4. Changes of the dispersion parameter of the suggested (PCF) with frequency at different (d = 140 μm, 150 μm, and 160 μm).

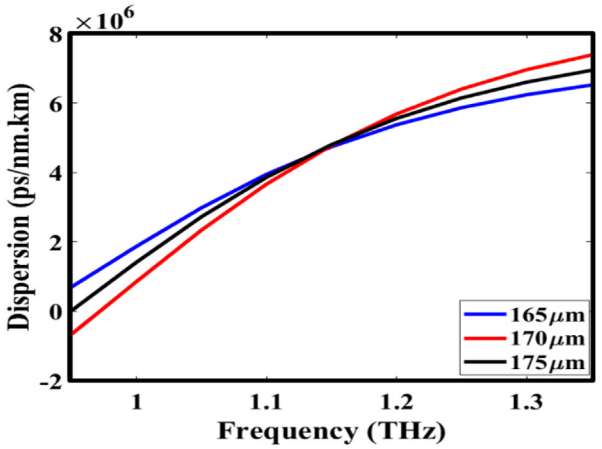

Fig. 5. Changes of the dispersion parameter of the suggested (PCF) with frequency at different [pitch = 165 μm, 170 μm, and 175 μm].

diameter of 140 μm, the highest effective area of about 0.76 μm^2, while the diameter of 150 μm shows a value of about 0.65 μm^2, and the diameter of 160 μm shows the lowest effective area of about 0.58 μm.

Fig. 7 shows the effect of distance pitch (Λ) variation on the effective area characteristics of an is fixed to fiber, diameter (d) = 150 micrometers, and three different pitch values of (165, 170, and 175) micrometers.When analyzing the specific values at 1 terahertz frequency, it can be revealed that the pitch Λ=175 micrometers the highest effective area of approximately 0.7 μm^2, while the pitch Λ=170 micrometers shows a value around 0.66 μm^2, and the pitch Λ=165 micrometers exhibits a slightly lower effective area of about 0.67 μm^2.

Fig. 8 shows the effect of diameter variation on the effective mode index characteristics of the optical fiber, pitch (Λ) = 170 micrometers, and three different diameters of (140, 150, and 160) μm,.When analyzing the specific values at 1 terahertz frequency, it can be revealed that the d = 140 μm diameter the highest effective mode index of approximately 1.31, while the d = 150 μm diameter

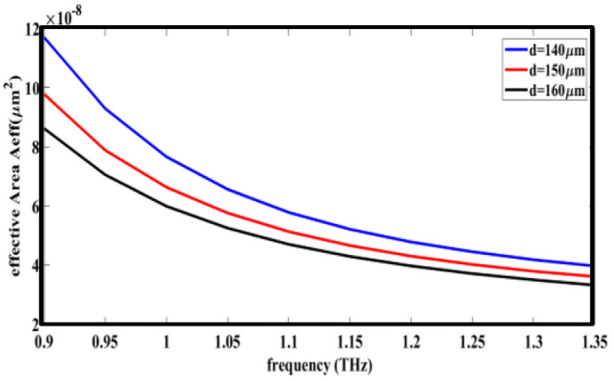

*Fig. 6. Changes of the effective area A_{eff} parameter of the suggested (PCF) with frequency at different (**d** = 140 μm, 150 μm, and 160 μm).*

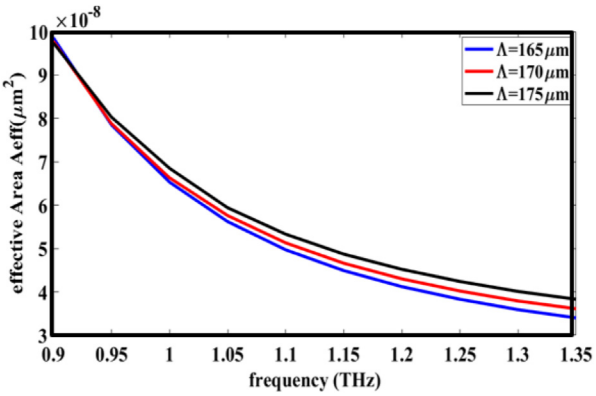

Fig. 7. Changes in the Effective Area the suggested (PCF's) parameter with frequency at various pitches (165 μm, 170 μm, and 175 μm).

shows a value around 1.29, and the d = 160 μm diameter exhibits a lower effective mode index of about 1.26.

Fig. 9 shows the effect of pitch (Λ) variation on the effective mode index characteristics of an optical fiber, in this study, diameter (d) = 150 micrometers, and three different pitch values of (165, 170 and 175) μm.It can be seen that pitch Λ=175 μm shows the highest effective mode index of approximately 1.31, while the pitch Λ=170 μm shows a value around 1.29, and the pitch Λ=165 μm exhibits a lower effective mode index of about 1.28 at the operating frequency 1THz.

When analyzing the specific values at 1 THz frequency, we find that the pitch Λ = 175 μm shows the highest effective mode index of approximately 1.32, while the pitch Λ = 170 μm shows a value around 1.30, and the pitch Λ = 165 μm exhibits a lower effective mode index of about 1.28.

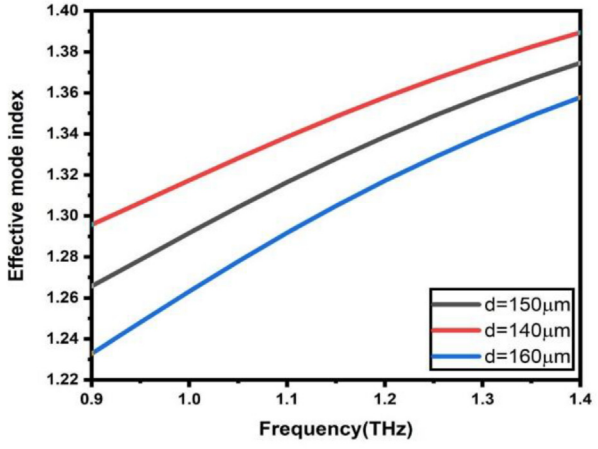

Fig. 8. Changes of the Effective mode index parameter of the suggested (PCF) with frequency at different (d = 140 μm, 150 μm, and 160 μm).

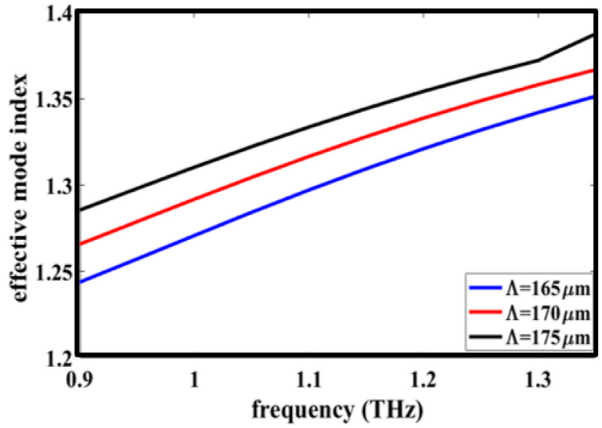

Fig. 9. Changes of the Effective mode index parameter of the suggested (PCF) with frequency at different (pitch = 165 μm, 170 μm, and 175 μm).

Numerous fabrication procedures, including the sol-gel casting method [17], drilling [18], and stack and draw method [19], can be used to create PCFs. The stack and draw method, which was first employed by Knight et al. [20], is the most often utilized technique for producing the PCF. Additionally, Chow et al. [5] have introduced a novel preform joining technique that makes use of the fiber drawing tower's furnace. In addition, various methods of selective filling are presented, such as capillary forces [21], UV glue sealing, and arc fusion deformation. Additionally, the authors in described a versatile technique for selective PCF filling with the aid of fs laser micromachining. PCF fabrication processes have significantly advanced, allowing for the effective implementation of complex PCF designs. For the core and cladding regions, lengthy tubes are initially made by melting several types of glass. These constructions are then subjected to precision casting. Once the tubes have set, they are carefully sliced into capillaries of different shapes. The capillaries and tubes are then ground and polished to a delicate smoothness as part of the mechanical refining process. The materials are then drawn at high temperatures to achieve the necessary dimensions. After that, the capillaries and other desired elements are placed into a preform. After that, the capillaries and other desired elements are placed into a preform. The preform's variable size and properties enable it to be arranged in a common lattice pattern, as illustrated in Fig. 1. In the last steps, a second cycle of the high-temperature drawing is necessary to produce the desired PCF. To preserve its integrity and boost its durability, the fibre is wrapped in a protective jacket, usually composed of a high-index polymer. Further, Atakaramians et al. [11] involve a two-step process

where preforms with macroscopic structures are first manufactured using extrusion techniques. The polymer material (TOPAS) is heated to 170–180 °C until soft, then forced through an extrusion die using a ram extruder. In the second step, the preform (10–15 mm diameter) is drawn down to fibers with outer diameters of a few hundred micrometers. The reported design employs similar dimensions to those proven successful in previous research, with hole diameters ranging from 140 to 160 μm and a core diameter of approximately 300 μm. These dimensions have been demonstrated to be achievable through current fabrication technologies.

This table specifically includes only research papers that used TOPAS material for THz PCF applications:

System	Dispersion (ps/THz·cm)	Effective Area (Aeff) (mm^2)	Nonlinearity ($W^{-1}\cdot m^2$)	Frequency (THz)
Nielsen et al. (2013) [22]	0.121.20.85 × 10^{-17} 0.3-1.0	1.2	0.85 × 10^{-17}	0.3–1.0
Islam et al. (2018) [19]	0.08	0.83	1.1 × 10^{-17}	0.7–1.2
Sultana et al. (2018) [23]	0.07	0.76	1.2 × 10^{-17}	0.8–1.2
Hasanuzzaman et al. (2016) [24]	0.06	0.55	1.3 × 10^{-17}	0.9–1.3
This work	0.05	0.45	1.4 × 10^{-17}	0.9–1.4

4. Conclusion

In this work, a porous core PCF is thoroughly studied. The pitch spacing and air hole diameter effect on the fiber's dispersion properties and effective mode index have been examined by varying them methodically. Our simulations show a strong relationship between these important parameters and the air hole diameter. The findings show that the fiber's characteristics can be tailored for particular uses, like maximizing the effective area or attaining low dispersion, by carefully adjusting the air hole diameter. These results offer important new information for future PCF-based device design and optimization for THz applications. The proposed fiber would have a great potential for terahertz in applications supercontinuum generation, THz sensing, and material substitutions.

Source of Funding

No funding received.

Conflict of Interest

No conflicts of interest related to this work.

Ethical Approval

Not applicable.

Data Availability

Publicly available data.

Author Contributions

All authors contributed equally to this work. Each author participated in the conceptualization, methodology, data analysis, and manuscript preparation.

Acknowledgment

We are grateful to the Department of Physics, College of Science, Al-Muthanna University for their assistance with this research work.

References

[1] Wang K, Mittleman DM. Metal wires for terahertz wave guiding. Nature 2004;432(7015):376–9.
[2] Reyes-Vera E, Usuga-Restrepo J, Jimenez-Durango C, Montoya-Cardona J, Gomez-Cardona N. Design of low-loss and highly birefringent porous-core photonic crystal fiber and its application to terahertz polarization beam splitter. IEEE Photon J 2018;10(4):1–13.
[3] Ho L, Pepper M, Taday P. Signatures and fingerprints. Nat Photonics 2008;2(9):541–3.
[4] Zhang L, Ren G, Yao J, Zhang Y. Design of the novel steering-wheel micro-structured optical fibers sensor based on evanescent wave of terahertz wave band. Optik 2014;125(20):5936–9.
[5] Sultana J, Islam MS, Faisal M, Islam MR, Ng BWH, Ebendorff-Heidepriem H, et al. Highly birefringent elliptical core photonic crystal fiber for terahertz application. Opt Commun 2018;407:92–6.
[6] Islam MS, Sultana J, Atai J, Abbott D, Rana S, Islam MR. Ultra low-loss hybrid core porous fiber for broadband applications. Appl Opt 2017;56(4):1232–7.
[7] Fukai C, Kurokawa K, Tajima K, Nakajima K, Sankawa I, Shinohara H. Long-term reliability of single-mode fibers when exposed to high-power laser light. J Lightwave Technol 2005;23(9):2713.
[8] Hansen TP, Broeng J, Libori SEB, Knudsen E, Bjarklev A, Jensen JR, et al. Highly birefringent index-guiding photonic crystal fibers. IEEE Photon Technol Lett 2001;13(6):588–90.
[9] Cregan R, Mangan BJ, Knight JC, Birks TA, Russell PSJ, Roberts PJ, et al. Single-mode photonic band gap guidance of light in air. Science 1999;285(5433):1537–9.
[10] Nielsen K, Rasmussen HK, Adam AJ, Planken PC, Bang O, Jepsen PU. Bendable, low-loss Topas fibers for the terahertz frequency range. Opt Express 2009;17(10):8592–601.
[11] Atakaramians S, Afshar V S, Ebendorff-Heidepriem H, Nagel M, Fischer BM, Abbott D. THz porous fibers: design,

fabrication and experimental characterization. Opt Express 2009;17(16):14053−62.
[12] Anthony J, Leonhardt R, Leon-Saval SG, Argyros A. THz propagation in kagome hollow-core microstructured fibers. Opt Express 2011;19(19):18470−8.
[13] Hameed MFO, Esmail MSM, Obayya SS. Terahertz photonic crystal fiber polarization rotator. J Opt Soc Am B 2020;37(10): 2865−72.
[14] Yakasai IK, Abas PE, Suhaimi H, Begum F. Low loss and highly birefringent photonic crystal fibre for terahertz applications. Optik 2020;206:164321.
[15] Kuiri B, Dutta B, Sarkar N, Santra S, Mandal P. Design and optimization of photonic crystal fiber with low confinement loss guiding 98 OAM modes in THz band. Opt Fiber Technol 2022;68:102752.
[16] Kuiri B, Dutta B, Sarkar N, Santra S, Mandal P, Mallick K, et al. Ultra-low loss polymer-based photonic crystal fiber supporting 242 OAM modes with high bending tolerance for multimode THz communication. Results Phys 2022;36:105465.
[17] Hasanuzzaman G, Rana S, Habib MS. A novel low loss, highly birefringent photonic crystal fiber in THz regime. IEEE Photon Technol Lett 2016;28(8):899−902.
[18] Islam R, Selim Habib M, Hasanuzzaman G, Rana S, Anwar Sadath M. Novel porous fiber based on dual-asymmetry for low-loss polarization maintaining THz wave guidance. Opt Lett 2016;41(3):440−3.
[19] Islam MS, Sultana J, Dinovitser A, Faisal M, Islam MR, Ng BWH, et al. Zeonex-based asymmetrical terahertz photonic crystal fiber for multichannel communication and polarization maintaining applications. Appl Opt 2018;57(4):666−72.
[20] Wu Z, Shi Z, Xia H, Zhou X, Deng Q, Huang J, et al. Design of highly birefringent and low-loss oligoporous-core THz photonic crystal fiber with single circular air-hole unit. IEEE Photon J 2016;8(6):1−11.
[21] Ahmed K, Paul BK, Chowdhury S, Sen S, Islam MI, Islam MS, et al. Design of a single-mode photonic crystal fibre with ultra-low material loss and large effective mode area in THz regime. IET Optoelectron 2017;11(6):265−71.
[22] Gan Z, Cao Y, Gu M. Direct laser writing of three-dimensional narrow bandgap and high refractive-index PbSe structures in a solution. Opt Express 2013;21(9):11202−8.
[23] Jiao X, Pan Q, Zhao X, Hao R, Bai X. Optical properties of monolayer polystyrene microspheres driven by a direct current. Opt Mater 2018;78:538−43.
[24] Zulkifli AZ, Latiff A, Paul MC, Yasin M, Ahmad H, Harun SW. Dual-wavelength nano-engineered Thulium-doped fiber laser via bending of singlemode-multimode-singlemode fiber structure. Opt Fiber Technol 2016;32:96−101.